

Analysis of Stability on the ERISA Humanoid Dance Robot

Bianca Surya Nobelia, Novian Fajar Satria, Eko Henfri Binugroho and Teuku Zikri Fatahillah
Politeknik Elektronika Negeri Surabaya, Jl. Raya ITS, Kampus PENS, Surabaya, Indonesia

Keywords: Humanoid Robot, Kinematics, ERISA, IMU Sensor, Analysis of Stability, Center of Mass.

Abstract: ERISA is a humanoid robot dancing developed by PENS students to participate in Indonesia Robot Contest (KRI) on the humanoid dancing robot division. One of the main assessments in this contest is to keep the robot stable until the finish zone. To analyze the stability of a humanoid robot, the Inertial Measurement Unit (IMU) sensor namely GY-952 is applied to detect the slope of the robot body. To determine the stability analysis variable of the robot, the Ground Projection of Center of Mass (GCoM) method is used by using the simplification of the Five Link Models. the ERISA robot starts to fall if there is an error approach around ± 40 mm. For future work, it is possible to apply it as feedback for a balance control system.

1 INTRODUCTION

The Indonesia robot contest has been held annually for more than a decade, one of the divisions in that contest is the Indonesia Dance Robot Contest (KRSTI). KRSTI is a competition for designing, manufacturing, and programming robots accompanied by elements of Indonesian art and culture, especially traditional dance in Indonesia. The purpose of this robot contest is to cultivate the students' creativity and interest in technological advances, especially in the industrial robotic field and traditional dance culture (KRI Committe, 2021).

One of the main assessments in this contest is to keep the robot stable until the finish zone. The difficult part is to keep the balance of the robot while performing dance movements and walking simultaneously. To overcome this, it is necessary to know about parameters of the stability of the robot before build a balancing system. Many studies were already conducted in this area, but in this paper present one of the easiest ways to analyze the stability of biped humanoid robotics by using an IMU sensor with a simplified Five-links model method. In order to prove this approach, the system was tested in three different conditions.

1.1 ERISA Robot Construction

The ERISA robot is designed using 29 servo motors arranged on an aluminum frame, PLA+, and using an ARM-type microcontroller as the main control



Figure 1: ERISA Robot Performance in KRSTI 2021.

system (Alasiry, Satria, & Sugiarto, 2018). The detail of the construction is explained below.

1.1.1 Mechanical Structure

ERISA robot design has 29 DoF (Degree of Freedom) consist of legs, body, hands, and head, as shown in Table 1 (Alasiry, Satria, & Sugiarto, 2018). Figure 3 shows the isometric view of the mechanical skeleton construction of the ERISA robot. Mechanical design has been done by using Autodesk Inventor® software and then the process of manufacturing parts is using CNC machines and a 3D Printer.

Table 1: DoF Part Detail on ERISA Robot.

| No. | Body Part | Amount of DoF |
|-------|-----------|--|
| 1. | Head | 3 (Neck) |
| 2. | Stomach | 1 (Stomach) |
| 3. | Waist | 1 (Waist) |
| 4. | Hand | 6 (Shoulder) 2 (Elbow) 4 (Wrist) |
| 5. | Feet | 6 (Hip) 2 (Knee) 4 (Ankle) |
| Total | | 29 DoF |

1.1.2 Electrical Design

To control the overall performance, ERISA utilizes STM32F407VGT as a microcontroller, it has a clock frequency up to 168MHz. The main controller runs robot performance ranging from kinematics calculations, accessing sensors, and communicating with other devices, in addition to more details can be seen in Figure 1. This microcontroller also performs the computation of the IMU data to access the roll, pitch, and yaw angle of the robot body (Alasiry, Satria, & Sugiarto, 2018). The orientation data will be received by the main microcontroller over UART communication.

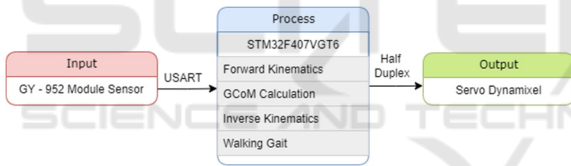


Figure 2: System Configuration Block Diagram.

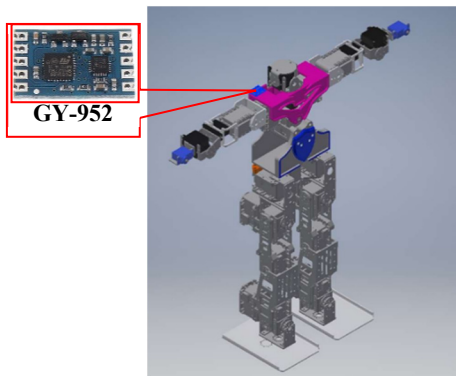


Figure 3: IMU Sensor Installation in the Robot Body.

1.1.3 IMU Sensor

The GY-952 module shown in Figure 3 is utilized as the IMU sensor in this research. The GY-952 module has a request-response communication model, so to

get the tilt data, the microcontroller must send a request command over UART communication and then wait for the response data. The microcontroller needs to parsing of the data packets that have been sent by the GY-952 module sensor. The placement of the IMU sensor is on the shoulder of the robot, because the shoulder of the robot is still in one connection with the trunk link of the robot.

2 SYSTEM OVERVIEW

There are two types of kinematics applied to the ERISA robot: forward kinematics and inverse kinematics. The forward kinematics is applied to control the movement of the hand servo and inverse kinematics for the leg. The forward kinematics is also used to enumerate the GCoM estimation.

2.1 Forward Kinematics

In general, forward kinematics is applied to find the End of Effector (EoE) position when all of the angle values in every joint are given. In this research, forward kinematics explanation will be focused to enumerate the GCoM estimation on the sagittal plane. The humanoid robot model is simplified to a Five-links model (Haavisto & Hyötyniemi, 2004) based on the link that has the most dominant mass. The humanoid Five-links model is shown in the following figure. The value of α_1 will be obtained from IMU sensor. While $\alpha_2, \alpha_3, \alpha_4, \alpha_5$ are the current angle of the servo.

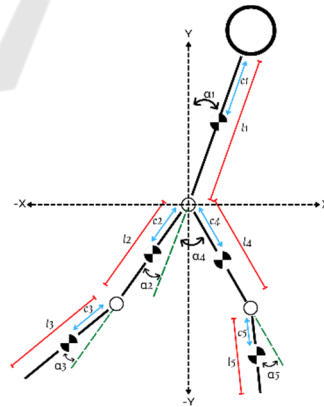


Figure 4: The Five-Links Model.

$$px_1 = l_1 \times \sin(\alpha_1) \quad (1)$$

$$px_2 = l_2 \times \sin(\alpha_1 + \pi + \alpha_2) \quad (2)$$

$$px_3 = px_2 + l_3 \times \sin(\alpha_1 + \pi + \alpha_2 + \alpha_3) \quad (3)$$

$$px_4 = l_4 \times \sin(\alpha_1 + \pi + \alpha_4) \quad (4)$$

$$px_5 = px_4 + l_5 \times \sin(\alpha_1 + \pi + \alpha_4 + \alpha_5) \quad (5)$$

$$py_1 = l_1 \times \cos(\alpha_1) \quad (6)$$

$$py_2 = l_2 \times \cos(\alpha_1 + \pi + \alpha_2) \quad (7)$$

$$py_3 = py_2 + l_3 \times \cos(\alpha_1 + \pi + \alpha_2 + \alpha_3) \quad (8)$$

$$py_4 = l_4 \times \cos(\alpha_1 + \pi + \alpha_4) \quad (9)$$

$$py_5 = py_4 + l_5 \times \cos(\alpha_1 + \pi + \alpha_4 + \alpha_5) \quad (10)$$

Where :

- l_i : Length of i^{th} link
- α_i : Joint angle of i^{th} link
- c_i : CoM position of i^{th} link
- px_i : EoE position of i^{th} link in X axis
- py_i : EoE position of i^{th} link in Y axis

2.2 Inverse Kinematics

The Inverse Kinematics used to resolve the walking trajectory in 3-Dimensional cartesian form. This inverse kinematic system is modeled on 6 DoF for each robot's leg, where the hip is managed as the base and the ankle as the End of Effector. The modeling calculation applies the triangle geometry solution. Cartesian coordinates are symbolized by the (x, y, z) axis, and for joints symbolized by the ($\alpha_1, \alpha_2, \alpha_3, \alpha_4, \alpha_5, \alpha_6$) degree. Figure 5 has illustrated the isometric shape of the robot leg configuration.

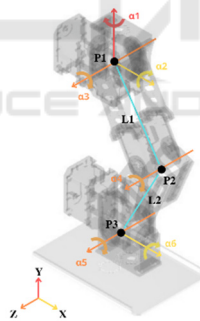


Figure 5: Joint Configuration on the Robot Leg (isometric view).

$$\alpha_1 = \theta_H \quad (11)$$

$$R0 = \sqrt{X^2 + Z^2}$$

Where :

- θ_H = Heading direction
- $R0$ = Resultant between X and Z value

As shown in Figure 5, joint 1 is directly affected by the heading direction.



Figure 6: Kinematics Model in Front View.

$$\beta = \tan^{-1}(Z/X) - \alpha_1$$

$$sZ = Z + (R0 \times \sin \beta)$$

$$sX = X - (R0 \times \cos \beta)$$

$$\alpha_2 = \tan^{-1}(sZ/\gamma)$$

$$R1 = \sqrt{\gamma^2 + sZ^2} \quad (12)$$

Where :

- β = Distance between R0 and sX
- sZ = Distance that occurs due to the angle β
- sX = Length of the hypotenuse of the triangles R0 and sZ
- α_2 = Angle between sZ and γ
- $R1$ = Resultant between sZ and γ



Figure 7: Kinematics Model in Side View.

The joint angle 2 can be obtained by referring to Figure 6. Where joint 2 is a plane that shows the side view, so that the robot's legs look like human legs.

$$R2 = \sqrt{R1^2 + sX^2}$$

$$\gamma C = \cos^{-1} \left(\frac{(L1^2 + L2^2 - R2^2)}{2 \times L1 \times L2} \right)$$

$$\gamma A = \sin^{-1} (X/R2)$$

$$\gamma B = \sin^{-1} (L2 \times \sin \gamma C / R2)$$

$$\alpha_3 = 0 - \gamma A + \gamma B \quad (13)$$

$$\alpha_4 = 180 - \gamma C \quad (14)$$

$$\alpha_5 = \alpha_3 - \alpha_4 \quad (15)$$

$$\alpha_6 = 0 - (\gamma A + \gamma B) \quad (16)$$

Where :

- L1 = Length of the upper leg
- L2 = Length of the lower leg
- R2 = Resultant between the R1 and sX
- γA = Angle between R2 and R1
- γB = Angle between R2 and L1
- γC = Angle between L1 and L2x
- α_3 = Angle from the sum of γA and γB
- α_4 = Angle of subtraction 180° and γC
- α_5 = Angle of the sum of α_3 and α_4
- α_6 = Reflection from angle α_2

After getting the values required for the calculations in Figure 5, another joint angle can be computed. From the inverse kinematics explanation above, eight coordinate data are acquired for moving the robot's legs, namely x, y, z, and headings, for the right foot and left foot, respectively (Alamri, 2020).

2.3 Walking Gait

This system utilizes a parabolic function trajectory pattern algorithm (walking path) with a set time interval, where the time interval is a parameter that can be changed (Alamri, 2020). The following trajectory equation is shown in equations (17) and (18).

$$\Delta S = PP - CP \tag{17}$$

$$\tilde{S}(t) = \sum_{t=0; t+n}^{180} \left((-\cos(t) + \frac{1}{2} \times \Delta S) + CP \right) \tag{18}$$

Where :

- ΔS = Difference between start and end positions
- PP = Previous Positions
- CP = Current Positions
- θ = Time Interval
- $\tilde{S}(t)$ = Output position at time (t)

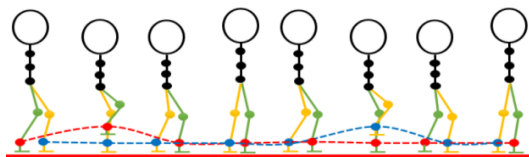


Figure 8: Inverse Kinematics of ERISA Robot.

The gait trajectory applied by ERISA to perform its walking sequence is 8 steps shown in Figure 8. The red color represents the right leg, while the blue color represents the left leg (Rahmawati, et al., 2021).

2.4 Motion Choreography

The dancing motion applied to the robot still uses trial and error tuning, as shown in the following flowchart.

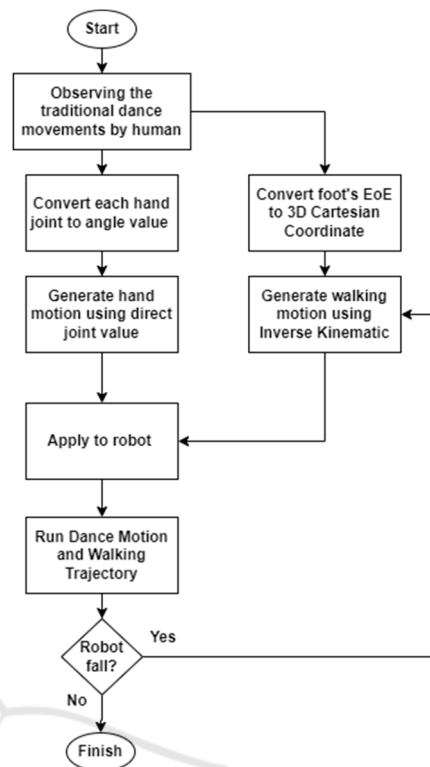


Figure 9: ERISA Robot's Tuning Method Flowchart.

Because the ERISA robot is still using an open-loop system, that's why when the robot falls, the walking trajectory must be corrected manually.

2.5 Ground Projection Center of Mass (GCoM)

The Center of Mass (CoM) is the point where the average mass of an object is equal to zero. All external forces and momentum will have an effect on the CoM of an object. Therefore in humanoid robots, CoM is utilized as a reference point to see the slope of the robot due to the force and momentum that occurs, which can be used as the error value (Nugroho, 2014). To keep the robot in balance the Ground Projection of the Center of Mass (GCoM) must be kept strictly inside the support polygon (Goswami, 1999).

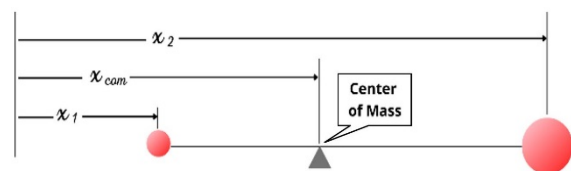


Figure 10: Center of Mass.

$$\begin{aligned}
 x_1 &= c_1 \times \sin(\alpha_1) \\
 x_2 &= c_2 \times \sin(\alpha_1 + \pi + \alpha_2) \\
 x_3 &= px_2 + c_3 \times \sin(\alpha_1 + \pi + \alpha_2 + \alpha_3) \\
 x_4 &= c_4 \times \sin(\alpha_1 + \pi + \alpha_4) \\
 x_5 &= px_4 + c_5 \times \sin(\alpha_1 + \pi + \alpha_4 + \alpha_5) \\
 GCoM &= \frac{\sum_{i=1}^n m_i x_i}{\sum_{i=1}^n m_i} \\
 GCoM &= \frac{m_1 x_1 + m_2 x_2 + m_3 x_3 + m_4 x_4 + m_5 x_5}{m_1 + m_2 + m_3 + m_4 + m_5}
 \end{aligned}$$

Where :

- m_i : Mass of i^{th} link
- x_i : GCoM position of i^{th} link in X-axis

3 RESULT

To analyze the stability of the robot using GCoM estimation, there are three different conditions applied to the robot, first is tracking GCoM position while the robot dancing and walking, second is while the robot dancing and doing one leg lifting motion, third is while the robot dancing and walking on obstacle. The data is taken by following the sequence as shown below.



Figure 11: System Design.

3.1 Tracking GCoM Position

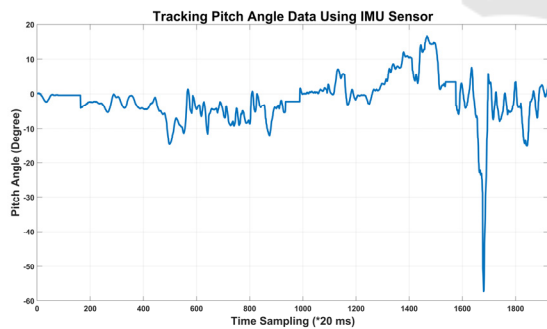


Figure 12: Tracking Pitch Angle Data using IMU Sensor.

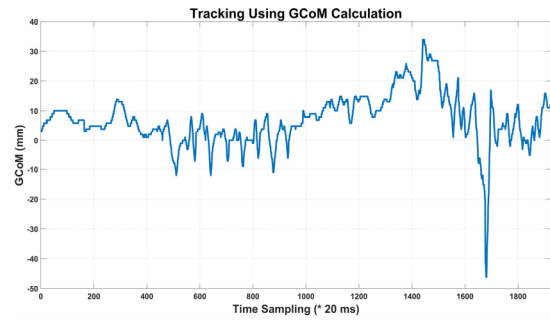


Figure 13: Tracking GCoM Position.

Figure 12 and Figure 13 are a comparison between tracking pitch data from the IMU sensor and tracking the GCoM position. The most basic difference occurs in GCoM calculation with Five-links model engaging the consideration while doing leg motion, whereas tracking pitch angle only uses data from the IMU sensor. There is a moment when the robot's posture is detected as an error, but it is still considered balanced based on its GCoM value. And vice versa, there is a moment when the robot's posture is detected as balanced by the IMU, but the motions can cause the robot to be unbalanced.

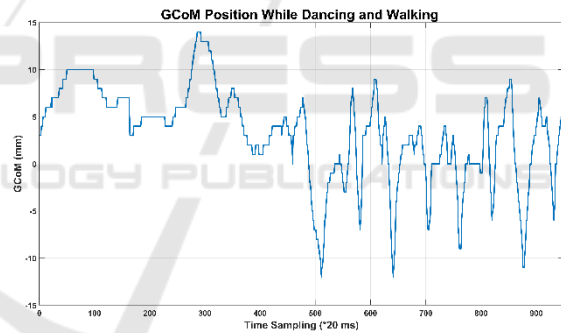


Figure 14: Graph of Tracking GCoM Position While the Robot Dancing and Walking.

Figure 14 unveils the experimental result while doing dance motions and walking. From the data above, the magnitude of the GCoM error with the reference (0 mm) make a fluctuation, which is up to 10 mm and less than -10 mm. This would cause the robot in an unstable condition.

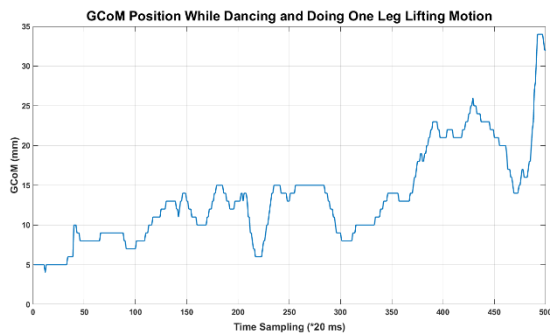


Figure 15: Graph of Tracking GCoM Position While the Robot Dancing and Doing One Leg Lifting Motion.

From the second condition, it can be inferred that carrying out one leg lifting motion will also cause the robot's body to be unstable. Although the GCoM error of the robot reaches 34 mm, it doesn't cause the robot fall. However, this situation make the robot easier to fall if there is any other disturbance.

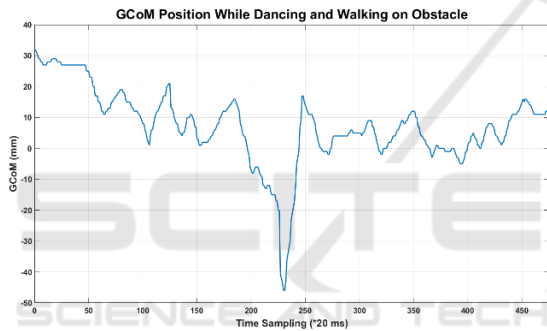


Figure 16: Graph of Tracking GCoM Position While the Robot Dancing and Walking on Obstacle.

Figure 16 shows that walking on the obstacle will cause the robot to fall backwards with a GCoM error around -40 mm. In other word, if the error value reaches approximately ± 40 mm, the robot no longer maintain its stability.

4 CONCLUSIONS

This study reveals one method to analyze the stability of a humanoid robot, which is by computing the position of the Center of Mass projected directly to the ground using a Five-links model. Calculating GCoM has more advantage than only using the angle value obtained from the IMU sensor, because it does not only consider the tilt of the robot's posture, but also the movements performed. Based on the experiments, the ERISA robot began to fall when the GCoM error reached the range of ± 40 mm. For future

works, it is possible to apply this analysis as feedback for balance control.

ACKNOWLEDGMENTS

This research is supported by the ERISA robotics team and Industrial Robotic Laboratory at Politeknik Elektronika Negeri Surabaya (PENS) (Rahmawati, et al., 2021).

REFERENCES

- Alamri, R. D. (2020). *Kontrol Keseimbangan Robot Humanoid ERISA Menggunakan PID Dengan Sensor Fusion*. Surabaya: Politeknik Elektronika Negeri Surabaya.
- Alasiry, A. H., Satria, N. F., & Sugiarto, A. (2018). Balance Control of Humanoid Dancing Robot ERISA while Walking on Sloped Surface using PID. *International Seminar on Research of Information Technology and Intelligent Systems (ISRITI)* (hal. 577-581). Yogyakarta: IEEE.
- Goswami, A. (1999). Postural Stability of Biped Robots and the Foot-Rotation Indicator (FRI) Point. *The International Journal of Robotics Research*, 523-533.
- Haavisto, O., & Hyötyniemi, H. (2004). *Simulation tool of a biped walking robot model*. Helsinki: Helsinki University of Technology.
- KRI Committe. (2021). Buku 5 Kontes Robot Seni Tari Indonesia (KRSTI) Daring 2021. *Petunjuk Pelaksanaan Kontes Robot Indonesia* (hal. 65-78). Jakarta: Pusat Prestasi Nasional Kementerian Pendidikan RI.
- Nugroho, A. T. (2014). *Optimalisasi Pergerakan dan Algoritma Robot Humanoid Sebagai Kiper*. Salatiga: Universitas Kristen Satya Wacana.
- Rahmawati, M. S., Irwansyah, A., Binugroho, E. H., Alasiry, A. H., Satria, N. F., & Basuki, D. K. (2021). ERISA Robot's Walking Trajectory Control using Pixy CMUcam5 to Locate the Target Position. *International Electronics Symposium (IES)* (hal. 476-481). Surabaya: IEEE.